Journal of Applied Physics

RESEARCH ARTICLE | JULY 15 2015

Electronic transitions and band offsets in C_{60}:SubPc and C_{60}:MgPc on MoO_3 studied by modulated surface photovoltage spectroscopy

S. Fengler; Th. Dittrich; M. Rusu

J. Appl. Phys. 118, 035501 (2015)
https://doi.org/10.1063/1.4926765

AIP Publishing

Electronic transitions and band offsets in C_{60}:SubPc and C_{60}:MgPc on MoO_3 studied by modulated surface photovoltage spectroscopy

S. Fengler, Th. Dittrich, and M. Rusu[a)]
Institut für Heterogene Materialsysteme, Helmholtz-Zentrum Berlin für Materialien und Energie, Lise-Meitner Campus, Hahn-Meitner-Platz 1, 14109 Berlin, Germany

(Received 21 April 2015; accepted 2 July 2015; published online 15 July 2015)

Electronic transitions at interfaces between MoO_3 layers and organic layers of C_{60}, SubPc, MgPc, and nano-composite layers of SubPc:C_{60} and MgPc:C_{60} have been studied by modulated surface photovoltage (SPV) spectroscopy. For all systems, time dependent and modulated SPV signals pointed to dissociation of excitons at the MoO_3/organic layer interfaces with a separation of holes towards MoO_3. The highest occupied molecular orbital (HOMO)-lowest unoccupied molecular orbital (LUMO) gaps (E_{HL}) of C_{60}, SubPc, and MgPc and the effective E_{HL} of SubPc:C_{60} and MgPc:C_{60} were measured. The offsets between the LUMO (ΔE_L) or HOMO (ΔE_H) bands were obtained with high precision and amounted to 0.33 or 0.73 eV for SubPc:C_{60}, respectively, and to −0.33 or 0.67 eV for MgPc:C_{60}, respectively. Exponential tails below E_{HL} and most pronounced sub-bandgap transitions were characterized and ascribed to disorder and transitions from HOMO bands to unoccupied defect states. © *2015 AIP Publishing LLC*.
[http://dx.doi.org/10.1063/1.4926765]

I. INTRODUCTION

Charge separation and transport at interfaces of solar cells are of basic importance for efficient devices. This task becomes even more striking for organic-inorganic hybrid solar cells. Illumination of organic semiconductors results in strongly bound excitons which should dissociate for charge separation in a solar cell. Excitons can dissociate into free charge carriers at interfaces with an appropriate band alignment between a material accepting electrons and a material donating electrons. In organic solar cells, excitons dissociate at donor-acceptor hetero-junctions.[1] The alignments of the highest occupied molecular orbitals (HOMOs) and of lowest unoccupied molecular orbitals (LUMOs) are essential for the effective dissociation of excitons in organic solar cells. It has been shown that the offsets of the HOMO and/or LUMO bands (ΔE_H and ΔE_L, respectively) should be slightly larger than the exciton binding energy which is of the order of 0.4 eV for organic semiconductors.[2]

Similar to donor/acceptor hetero-junctions, ultra-fast photo-induced charge transfer can also occur across interfaces between organic semiconductors and metal oxide semiconductors with wide band gaps such as SnO_2, TiO_2, and ZnO.[3] Thus, the investigation of charge transfer and dissociation of excitons are important for both organic/organic and organic/inorganic interfaces. This is also of interest for the design of hybrid solar cells based on nano-composites with metal oxide nano-particles embedded in an organic matrix[3] or with organic molecules infiltrated into a nano-structured metal oxide scaffold.[4] Especially, the transition metal oxides are of great interest in composite absorber layers[5] or as anodes in organic solar cells.[6] In the last few years, MoO_3 attracted attention as a transition metal oxide for electrodes. The band gap of MoO_3 ranges between 3.1 and 4.1 eV depending on the phase[7,8] and MoO_3 has a high work function usually between 5.3 (Ref. 9) and 5.5 eV.[8] The corresponding energies of the conduction and valence band edges (E_c and E_v, respectively) of MoO_3 are between 2.3 (Ref. 9) and 2.5 eV (Ref. 10) and between 5.3 and 5.7 eV, respectively. As remark, values of a work function, E_c and E_v of 6.86, 6.7, and 9.68 eV, respectively, were reported as well for MoO_3.[5] In this work, MoO_3 layers will be used as substrates.

Electronic states below the HOMO-LUMO gap and disorder cause localization and are therefore crucial for the limitation of charge transfer across interfaces and charge transport, for example, due to hopping.[11–13] Mechanisms of charge transport depend sensitively on the structure and local disordering[14] causing a random distribution of potentials and a distribution of densities of localized states.[15] Exponentially distributed defect states below a band gap are a typical signature for disorder. Weak intermolecular interactions caused by van-der-Waals binding have important consequences for disorder and therefore for the electronic properties of organic semiconductors deposited, for example, on rough surfaces.

As an exceptional electron acceptor, fullerene (C_{60}) is the most commonly used acceptor molecule in organic solar cells.[16] The electron or hole mobilities of layers of C_{60} molecules (C_{60} layers) are between 5×10^{-2} and 1 $cm^2/V\,s$ (Refs. 17 and 18) of about 10^{-4} $cm^2/V\,s$,[18] respectively. The transfer of electrons from an excited donor into C_{60} occurs within about 40 fs.[19] The exciton diffusion length and the values of E_H and E_L are of the order of 40 nm (Ref. 20) and 6.2 and 4.5 eV, respectively, in C_{60} layers.[21] The absorption coefficient of C_{60} layers reaches 8×10^4 cm^{-1} in the wavelength range between 400 and 500 nm.[22]

[a)]Author to whom correspondence should be addressed. Electronic mail: rusu@helmholtz-berlin.de. Tel.: +49 30 8062 42604. Fax: +49 30 8062 43199.

A large variety of donor molecules are used in combination with C_{60} molecules in organic solar cells. Among them, small molecules such as SubPc (sub-phthalocyanine) and MgPc (Mg-phthalocyanine) are of interest. SubPc has the potential for increasing the open circuit voltage in organic solar cells due to the relatively large HOMO-LUMO gap. The values of E_H and E_L are 5.6 and 3.6 eV, respectively, for layers of SubPc molecules.[23] The absorption coefficients of SubPc or MgPc layers are as high as $3 \times 10^5\,cm^{-1}$ between 450 and 650 nm.[24] The absorption of MgPc is extended to a range up to 850 nm and the values of E_H and E_L are 5.4 and 3.9 eV, respectively.[25]

This work aims to the investigation of the dissociation of excitons at interfaces between layers of MoO_3 and C_{60}, SubPc, and MgPc, as well as between layers of MoO_3 and composite layers of SubPc:C_{60} and MgPc:C_{60}. Charge separation caused by the dissociation of excitons has been detected by spectral dependent surface photovoltage (SPV) measurements. Transition energies related to the HOMO-LUMO gaps, disorder and to sub-bandgap levels, and impurity bands are obtained. The values of ΔE_H and ΔE_L, are deduced for the composite layers of MgPc:C_{60} and SubPc:C_{60}. The results demonstrate that SPV measurements can be easily applied for a direct characterization of electronic properties of organic semiconductors and of interfaces in layers systems with organic semiconductors.

II. MATERIALS AND METHODS

A. Thin film preparation

Layers of MoO_3 were deposited onto planar glass substrates coated with ITO (Präzisions Glas&Optik GmbH) by thermal evaporation from a stoichiometric source. The base pressure in the evaporation chamber and the deposition rate were 5×10^{-7} mbar and 0.02 nm/s, respectively. The thickness of the MoO_3 layers was 7 nm. The work function of the prepared MoO_3 layers was characterized by Kelvin probe force microscopy and amounted to 5.3 eV.

Organic layers of C_{60}, SubPc, MgPc, SubPc:C_{60}, and MgPc:C_{60} were deposited by organic vapor phase deposition (OVPD)[26,27] with nitrogen as a carrier gas at a pressure of about 0.6 mbar (setup by AIXTRON). The temperatures of the C_{60}, SubPc, and MgPc sources were kept at 436, 330, and 424 °C, respectively. The flow rates through sources were adjusted in such a way that a deposition rate of 0.05 nm/s was reached for the separate organic molecules. The total flow rate across the deposition chamber was 1150 sccm. The substrate temperature during deposition was 150 °C. The thickness of the deposited organic layers was 45 nm. The samples were stored in nitrogen before performing SPV measurements.

B. Characterization

The surface and bulk electronic properties of investigated material systems were studied by the SPV method which is a well-established contactless technique for the characterization of semiconductors and relies on analyzing illumination-induced changes in the surface voltage.[28] The SPV signal is expressed by the equation

$$SPV = \frac{d}{\varepsilon \cdot \varepsilon_0} \cdot Q, \tag{1}$$

where the charge separation length, d, corresponds to the distance between the centers of the positive and negative charge carriers with the areal density Q.[26,29] The symbols ε and ε_0 denote the relative dielectric constant and the dielectric constant of vacuum, respectively. The values of d and Q are functions of time (t) and position (x) and depend in a complex way on the generation rate and transport and recombination processes.

SPV measurements were performed in vacuum at $\sim 10^{-2}$ mbar (spectral dependent measurements) and $\sim 10^{-5}$ mbar (transient measurements). A schematic of the experimental setup joining both is shown in Figure 1(a). The total exposure time of the samples to air was less than 1 min.

SPV measurements were carried out in the fixed capacitor arrangement.[30] The capacitor was formed between the organic layer and the quartz electrode coated with SnO_2:F by introducing a mica sheet (thickness about 30 μm). The electrode was gently pressed with a cardanic spring onto the mica placed on the sample (pressure about 5 N/cm^2, see also Figure 1(a)). The input resistance of the high impedance buffer was 50 GΩ, so that a RC time constant of the order of 1 s was reached. SPV transients were excited with single pulses of a tunable Nd:YAG laser (EKSPLA, NT 342/1/UVE). The wavelength and the duration time of a laser pulse

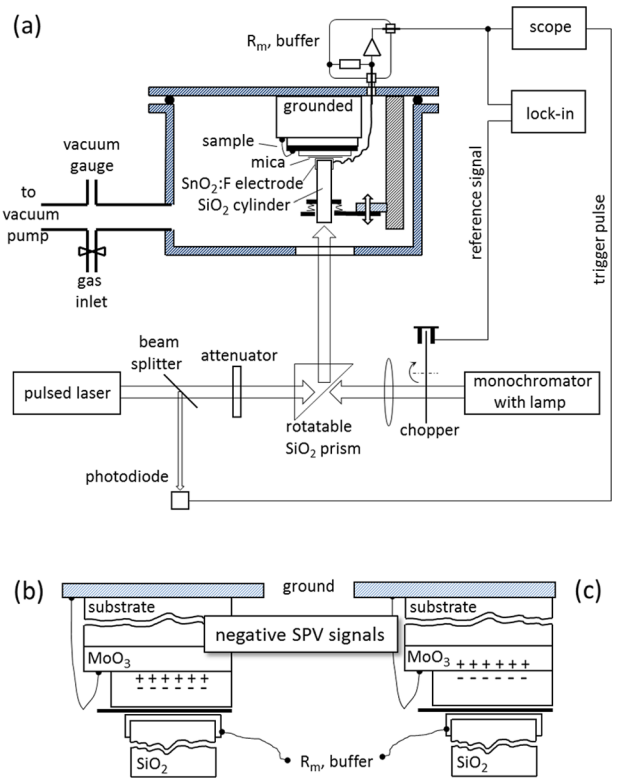

FIG. 1. Schematic of the merged experimental setup (a) and schematic film structure with separated charge carriers giving a negative surface photovoltage signal in the case that holes are separated in front of the MoO_3 layer (b) or into the MoO_3 layer (c).

were 500 nm and 5 ns, respectively. A sampling rate of 10 ns was chosen. SPV transients were recorded with a sampling oscilloscope (GAGE CS14200) by applying a logarithmic read-out.[31] A halogen lamp with a quartz prism monochromator (SPM2) and an optical chopper (modulation frequency 8 Hz) was applied for spectral dependent modulated SPV measurements with a lock-in amplifier (EG&G 7260).

III. RESULTS AND DISCUSSION

A. Charge separation

Figure 2 shows the SPV transients measured for C_{60}/MoO_3, SubPc/MoO_3 and SubPc:C_{60}/MoO_3 structures. All transients had a negative sign indicating that photo-generated electrons were separated towards the front surface whereas photo-generated holes were separated towards the MoO_3 thin film (see also the schemes in Figures 1(b) and 1(c)).

For C_{60}/MoO_3, the maximum of the SPV signal appeared within the resolution time of the system after excitation. The relaxation of the SPV signal of C_{60}/MoO_3 was characterized by a fast decrease from about −0.13 V to about −0.08 V within the first 10–20 ns and by a slow relaxation within about a second. For SubPc/MoO_3, the SPV signal reached about −0.075 V within the first 20 ns, increased to about −0.11 V after 4 μs and decreased in the following very slowly. For SubPc:C_{60}/MoO_3, the SPV signal reached about −0.10 V within the first 20 ns, increased to about −0.13 V after 9 μs and decreased in the following very slowly as well.

The SPV transients were caused by dissociation of excitons at the organic layer/MoO_3 interface with a separation of holes towards the MoO_3. Long relaxation times can be explained by trapping of electrons in the organic layer before recombining with holes at the surface of the MoO_3 layer.

The retardation of the maximum of SPV transients corresponds often to charge transport due to diffusion leading to an increase of the distance between the centers of positive and negative charge.[32] At first glance, the time at which the SPV signal reached its maximum can be related to the dielectric relaxation time[33] depending on the reciprocal conductivity and therefore on the reciprocal electron mobility. The mobility of electrons in C_{60} layers, for example, is about 0.5–1.0 cm^2/V s in the case of sublimed and molecular beam deposited films[18,34] and up to 5 cm^2/V s in the case of deposition onto molecular-wetting controlled substrates.[35] In contrast, the electron mobility in metal phthalocyanine (MPc) layers is by 3–4 orders of magnitude lower in comparison to C_{60} layers.[36]

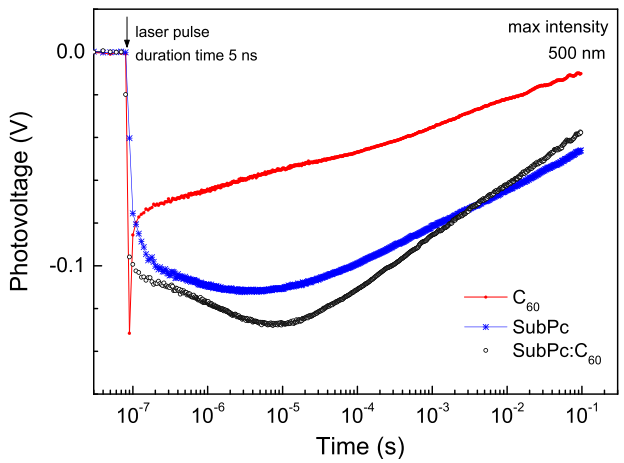

FIG. 2. Surface photovoltage transients of C_{60}/MoO_3 (red circles), SubPc/MoO_3 (blue stars), and SubPc:C_{60}/MoO_3 (open circles). The transients were excited with single laser pulses with duration time of 5 ns at the wavelength of 500 nm. The arrow marks the time at which the laser pulse was switched on.

B. HOMO-LUMO gaps

The measurement of a HOMO-LUMO gap with modulated SPV spectroscopy is not straight forward since different electronic states can give different contributions to the SPV signal regarding signs and values. Transition energies can be investigated by SPV with high precision if the sign of the SPV signal does not change in the region of the transition. As shown by the SPV transients, the sign of the SPV signals did not change for all samples over the investigated a time interval from 10 ns to 1 s. As an example, Figure 3 shows modulated in-phase and phase-shifted by 90° SPV spectra of the SubPc/MoO_3 sample. The in-phase (x) and phase-shifted by 90° (y) SPV signals were negative and positive, respectively, over the whole spectral range. Therefore, the direction of separation of photo-generated electrons was independent of the time scale and of the kind of excitation. The SPV signals set on at photon energies of about 1 eV and increased strongly at photon energies between 1.8 and 2.0 eV which is related to the region of the HOMO-LUMO gap of SubPc. The SPV signals decreased strongly at photon energies between 2.2 and 2.8 eV. A second peak appeared at about 3.4 eV.

Onset energies of SPV signals can be defined as the photon energy at which the tangent in the turning point reaches zero (see the dashed lines in Figure 2). In the region of the HOMO-LUMO gap of SubPc, the onset energies of the x- and y-signals amount to 1.91 and 1.84 eV, respectively. The fact that the onset energies are different for the x- and y-signals shows that different electronic states are probed near the

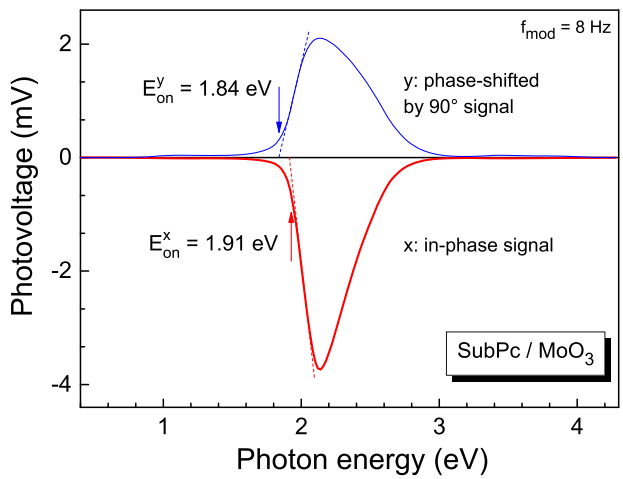

FIG. 3. Modulated in-phase (thick red line) and phase-shifted by 90° (thin blue line) surface photovoltage spectra of SubPc deposited onto MoO_3. The arrows mark the onset energies.

HOMO-LUMO gap. The point is that the in-phase signal follows the modulation, i.e., the x-signal is sensitive to fast processes in relation to the modulation period. In contrast, the phase-shifted by 90° signal is retarded in relation to the modulation, i.e., the y-signal is sensitive to slow processes in relation to the modulation period.

The ratio between the y- and x-signals, also called tangent of the phase angle, changes in the range around the HOMO-LUMO gap. Figure 4(a) depicts the dependence of the phase angle on the photon energy. The phase angle increased from about 113° at 1.7 eV to about 150° at 2.1 eV. An increase of phase angles between 90° and 180° and a decrease of phase angles between 0° and 90° mean that the modulated charge separation becomes faster in relation to the modulation period. In disordered semiconductors, trapping limits phenomena related to transport. Charge carriers trapped in the deepest traps have the longest trapping times. Therefore, permanent filling of the deepest traps leads to faster transport of photo-generated charge carriers.

The PV amplitude is defined as the square root of the sum of the squared x- and y-signals. Near the HOMO-LUMO gap, an increase of the PV amplitude is related to the increase of the photo-generation rate and therefore to the increase of the density of photo-generated charge carriers. As a consequence, more and more deep traps are getting filled with increasing PV amplitude, so that the SPV signals can follow faster and faster the modulation. The resulting increase of the phase angle towards 180° with increasing PV amplitude can be clearly seen in Figure 4(b).

The absolute x- and y-signals are plotted together with the PV amplitude in Figure 5 in a semi-log scale for the range near the HOMO-LUMO gap of SubPc. The spectrum of the photon flux is shown for comparison. The absolute values of the x- and y-signals changed over more than one order of magnitude in the given range. Near the HOMO-LUMO gap, the spectra were fitted with exponentials. The characteristic energies of the so-called tails amounted to 0.056, 0.083, and 0.073 eV for E_t^x, E_t^y, and E_t^R, respectively. As remark, a slower response corresponds to emission from deeper trap states. Therefore, it is not surprising that E_t^y was

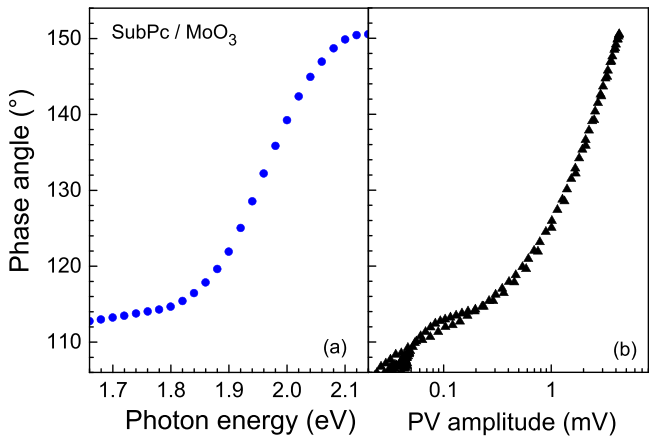

FIG. 4. Dependence of the phase angle on the photon energy (a) and on the PV amplitude (b) for SubPc/MoO_3.

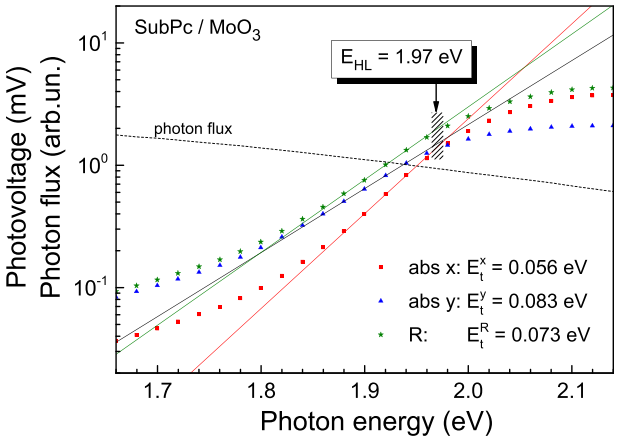

FIG. 5. Spectra of the absolute PV x- and y-signals (red rectangles and blue triangles, respectively) and of the PV amplitude (green stars) and of the photon flux (dashed line) in the region near the HOMO-LUMO gap of SubPc/MoO_3. The solid red, blue, and green lines are exponentials with the characteristic energies of 0.056, 0.083, and 0.073 eV for E_t^x, E_t^y, and E_t^R, respectively. The arrow marks the HOMO-LUMO gap of SubPc/MoO_3.

larger than E_t^{yx} and that the onset energy was larger for the x-signals than for the y-signals.

Usually, SPV spectra are not divided by the photon flux since SPV signals depend on several parameters being influenced by the photon flux as well. If assuming a linear dependence of the SPV signals on the generation rate for the given spectra, the values of E_t^x, E_t^y, and E_t^R would reduce to 0.05, 0.07, and 0.063 eV, respectively, after correcting to the photon flux. In this sense, an uncertainty in the values of E_t^x, E_t^y, and E_t^R of the order of 10%–20% should be taken into account.

If considering disorder, the value of the HOMO-LUMO gap can be defined as the photon energy at which the SPV spectrum starts to deviate from the exponential. For SubPc, this happened between 1.96 and 1.98 eV, i.e., the HOMO-LUMO gap was about 1.97 eV. As remark, this value was very similar for the x- and y-signals and significantly larger than the values of the on-set energies.

The qualitative behavior of the SPV spectra was similar for all samples. Therefore, all spectra have been treated in the same way shown above. The spectra of the PV amplitude of C_{60}/MoO_3, SubPc/MoO_3 and SubPc:C_{60}/MoO_3 are compared in Figure 6. The PV amplitude reached a maximum at about 2.4 eV for C_{60}/MoO_3 and at about 2.1 eV for SubPc/MoO_3 and SubPc:C_{60}/MoO_3. In the maximum, the values of the PV amplitude amounted to about 0.11, 4.3, and 13 mV for C_{60}/MoO_3, SubPc/MoO_3 and SubPc:C_{60}/MoO_3, respectively. As remark, peak positions of PV amplitudes can differ for different samples since PV amplitudes of different samples can depend differently on parameters controlling photo-generation, charge transport, trapping, and recombination processes. Therefore, peak positions have not been analyzed.

The observed signals indicate an effective dissociation of excitons at the organic/inorganic interface. The recorded SPV signal was much higher for the SubPc:C_{60}/MoO_3 sample due to the strong contribution of the SubPc:C_{60} interface where excitons are separated as well, whereas resulting free

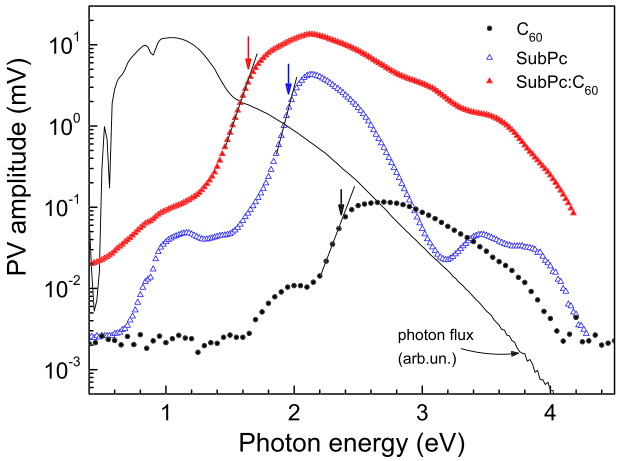

FIG. 6. Spectra of the PV amplitude of C_{60}/MoO_3 (black circles), SubPc/MoO_3 (open blue triangles), and SubPc:C_{60}/MoO_3 (filled red triangles). The spectrum of the photon flux is shown for comparison. The arrows mark the HOMO-LUMO gaps.

charge carriers are separated in the same direction. The HOMO-LUMO gap was 2.37 eV for the C_{60} layer and the value of E_t^R amounted to 0.11 eV. For SubPc:C_{60}/MoO_3, the values of E_{HL} and E_t^R were 1.64 and 0.097 eV, respectively.

The spectra of the PV amplitude of MgPc/MoO_3 and MgPc:C_{60}/MoO_3 are compared in Figure 7 to that of C_{60}/MoO_3. In contrast to SubPc, the PV maximum amplitudes were much lower for MgPc/MoO_3 (0.18 mV at 1.52 eV) and MgPc:C_{60}/MoO_3 (0.26 mV at 1.78 eV). Moreover, the PV amplitude of MgPc:C_{60}/MoO_3 was only slightly higher compared to that of MgPc/MoO_3. This shows that the MgPc/C_{60} interface is not effective for dissociation of excitons. Further, the values of the HOMO-LUMO gap were 1.37 eV (MgPc/MoO_3) and 1.70 eV (MgPc:C_{60}/MoO_3). The HOMO-LUMO gap was 1.37 eV for the MgPc layer and the value of E_t^R amounted to 0.068 eV. For MgPc:C_{60}/MoO_3, the values of E_{HL} and E_t^R were 1.70 and 0.25 eV, respectively. Table I summarizes the values of E_{HL} for the different layers and layer systems.

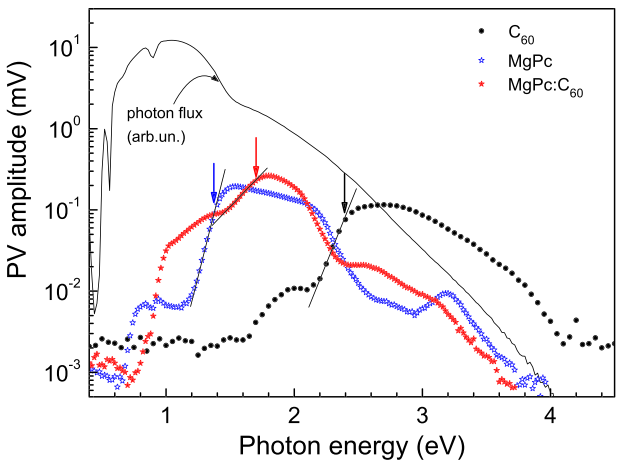

FIG. 7. Spectra of the PV amplitude of C_{60}/MoO_3 (black circles), MgPc/MoO_3 (open blue stars), and MgPc:C_{60}/MoO_3 (filled red stars). The spectrum of the photon flux is shown for comparison. The arrows mark the HOMO-LUMO gaps.

TABLE I. HOMO-LUMO gap energies (E_{HL}) and sub-bandgap energies (E_{SB}) for bare C_{60}, SubPc, and MgPc as well as for SubPc:C_{60} and MgPc:C_{60} nano-composites. For nano-composites, the HOMO- and LUMO-offsets (ΔE_H and ΔE_L) are shown.

Thin film	E_{HL} (eV)	E_{SB} (eV)	ΔE_L (eV)	E_H (eV)
C_{60}	2.37	1.85		
SubPc	1.97	0.96		
MgPc	1.37	0.75		
SubPc:C_{60}	1.64	0.96	0.33	0.73
MgPc:C_{60}	1.70	1.00	−0.33	0.67

C. HOMO and LUMO offsets

The value of the work function of MoO_3 is in good agreement with the direction of the separation the positive charge to the metal oxide after dissociation of excitons at interfaces between C_{60}, SubPc, SubPc:C_{60}, and MoO_3.

The values of E_{HL} for the organic single layers and for the organic nano-composite layers can be used to determine the band offsets between the HOMO (ΔE_H) and LUMO (ΔE_L) bands of the organic components in the nano-composite. The values determined in Sec. III B for $E_{HL}(C_{60})$, E_{HL}(SubPc), E_{HL}(SubPc:C_{60}), E_{HL}(MgPc), and E_{HL}(MgPc:C_{60}) are equal to 2.37, 1.97, 1.64, 1.37, and 1.70 eV, respectively.

During dissociation of excitons at donor acceptor hetero-junctions, electrons are separated into C_{60}, i.e., the energy of the LUMO band of C_{60} is lower than the energy of the LUMO bands of SubPc or MgPc (see also Figure 8). Therefore, the corresponding HOMO and LUMO band offsets can be obtained by using the following equations:

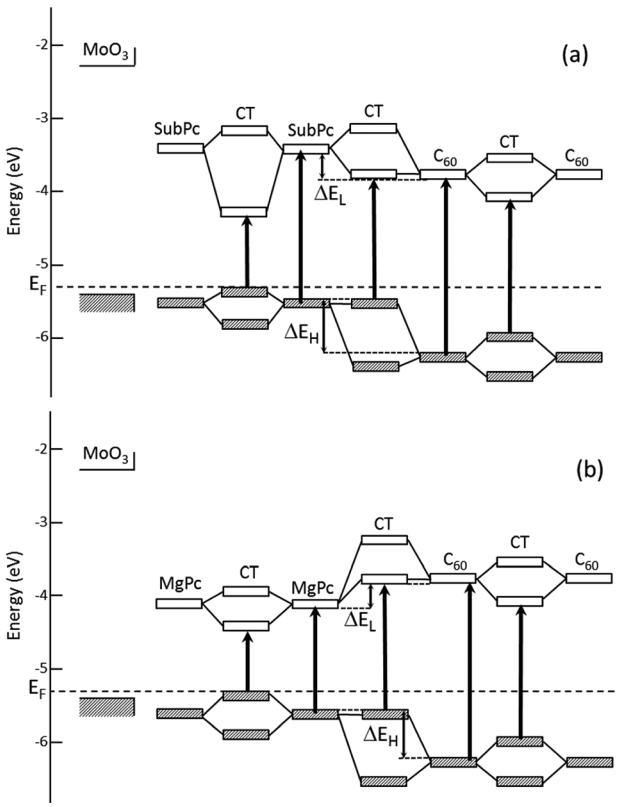

FIG. 8. Schematic of energy levels and transitions in SubPc:C_{60} (a) and MgPc:C_{60} (b). The levels are aligned with respect to the HOMO level of C_{60}.[22,24]

$$E_H(SubPc - C_{60}) = E_{HL}(C_{60}) - E_{HL}(SubPc : C_{60}), \quad (2)$$

$$E_L(SubPc - C_{60}) = E_{HL}(SubPc) - E_{HL}(SubPc : C_{60}), \quad (3)$$

$$E_H(MgPc - C_{60}) = E_{HL}(C_{60}) - E_{HL}(MgPc : C_{60}), \quad (4)$$

$$E_L(MgPc - C_{60}) = E_{HL}(MgPc) - E_{HL}(MgPc : C_{60}). \quad (5)$$

The band offsets can be interpreted in terms of charge transfer states coupling with the corresponding HOMO or LUMO band as shown in Figure 8. The values of the HOMO and LUMO band offsets determined with the help of Eqs. (2)–(5) are equal to 0.73, 0.33, 0.67, and −0.33 eV for ΔE_H(SubPc-C_{60}), ΔE_L(SubPc-C_{60}), ΔE_H(MgPc-C_{60}), and ΔE_L(MgPc-C_{60}), respectively (see also Table I). For comparison, the HOMO energies (E_H) are, with respect to the vacuum energy, of about 6.2 eV (Refs. 21 and 23) for C_{60}, about 5.6 eV for SubPc (Ref. 23) and approximately 5.4 eV (Ref. 25) for MgPc resulting in values of 0.6 eV for ΔE_H(SubPc-C_{60}) and 0.49 eV for ΔE_H(MgPc-C_{60}). The values of ΔE_H obtained for the organic nano-composites by modulated SPV spectroscopy correspond well to the ranges which have been obtained from photoelectron spectroscopy measurements on the corresponding organic single layers. Figure 7 depicts the HOMO and LUMO energies with the corresponding band offsets obtained from the SPV data, whereas the HOMO energy of C_{60} (6.2 eV) has been considered for reference.

The SubPc-C_{60} interface is charge-selective in the sense that the potential energies of electrons or holes are lower in the LUMO band of C_{60} or in the HOMO band of SubPc, respectively. In contrast, the potential energies of electrons or holes have a minimum in the LUMO or HOMO bands, respectively, of MgPc for the MgPc-C_{60} interface. Therefore, it is not surprising that the modulated PV amplitude increased much stronger and over the whole spectral range for the SubPc:C_{60} than for the MgPc:C_{60} nano-composite.

D. Transitions at lower photon energies

There are pronounced features in the SPV spectra in Figures 6 and 7 at photon energies below the energies of HOMO-LUMO transitions. These features can be ascribed to characteristic sub-bandgap energies (E_{SB}) which can be determined similarly as the values of E_{HL} (see also Figure 8). The corresponding values of E_{SB}(C_{60}), E_{SB}(SubPc), E_{SB}(SubPc:C_{60}), E_{SB}(MgPc), E_{SB}(MgPc:C_{60}), and E_{SB}(MgPc:C_{60}) are 1.85, 0.96, 0.96, 0.75, and 1.00 eV, respectively. The origin of SPV signals below the HOMO-LUMO transition has been recently discussed by Osterloh *et al.*[37,38] Localization of charge carriers in layers of conjugated molecules causes the formation of charge transfer states within the HOMO-LUMO gap.

The Fermi-level and the energy of the MoO_3 conduction band edge are well above the HOMO bands of C_{60}, SubPc, and MgPc. For this reason, the overall direction of charge separation is given by transfer of photo-generated holes from the HOMO bands of the organic semiconductors into MoO_3. Furthermore, photo-excitation of electrons from the HOMO bands of the organic semiconductors into MoO_3 does not take place since only positive charges are detected on MoO_3.

The sub-bandgap energies in SubPc and MgPc are quite close to the middle of the HOMO-LUMO gaps. Therefore, in addition to the formation of charge transfer states, E_{SB}(SubPc) and E_{SB}(MgPc) may be caused as well by transitions from states in the HOMO band into unoccupied defect states or from occupied defect states into states in the LUMO band. Transitions being related to E_{SB} of C_{60}, MgPc and SubPc were also found in absorption spectra, i.e., the pronounced transitions measured by SPV are not related to the formation of charge transfer states at the organic/MoO_3 interfaces. However, if taking a closer look at the SPV spectra, more than only the well pronounced transitions can be distinguished and it cannot be excluded that charge transfer states at the organic/MoO_3 interfaces are involved.

All the characteristic energies determined in this work for bare C_{60}, SubPc, MgPc as well as for SubPc:C_{60} and MgPc:C_{60} nano-composites are summarized in Table I.

IV. CONCLUSION

We have studied the separation of charge carriers at interfaces formed between MoO_3 inorganic thin films and organic layers of C_{60}, SubPc, MgPc, and nano-composite layers of SubPc:C_{60} and MgPc:C_{60}. The investigations were performed by using SPV for the determination of material and interface electronic properties in structures as applied in organic solar cells. We observe for all layer systems that photo-generated excitons dissociate at the MoO_3/organic layer interfaces and the corresponding electrons and holes separate into the organic layer and MoO_3, respectively. As a consequence, the introduction of MoO_3 nanoparticles into hybrid organic:inorganic absorber thin films of photovoltaic devices can effectively contribute to the dissociation of photo-generated excitons and charge separation. In blend films that contain C_{60}, an effective dissociation of excitons is observed only on structures that comprise SubPc. For this case, a LUMO-offset of 0.33 eV and a HOMO-offset of 0.73 eV is found. In contrast, the combination of C_{60} with MgPc is not effective for dissociation of excitons. This is caused by a large negative value of ΔE_H and a large positive value of ΔE_L (−0.33 eV and 0.67 eV, respectively).

The energies of the HOMO-LUMO gaps (2.37, 1.97, and 1.37 eV for C_{60}, SubPc, and MgPc, respectively) and of the effective HOMO-LUMO gaps (1.64 and 1.70 eV for SubPc:C_{60} and MgPc:C_{60}, respectively) were determined as the energies at which the SPV signals begin to decrease exponentially with decreasing photon energy. The exponential decrease of the SPV signals with decreasing photon energy, i.e., the tails of the HOMO and/or LUMO bands, has been ascribed to disorder of molecules in the investigated organic layers. The sub-bandgap transitions observed at 1.85 eV, 0.96 eV, and 0.75 eV in C_{60}, SubPc, and MgPc, respectively, have been ascribed to transitions from the HOMO bands to unoccupied defect states.

ACKNOWLEDGMENTS

The authors gratefully acknowledge Helmholtz-Gemeinschaft Deutscher Forschungszentren e.V. (HGF) (Project "Hybrid-PV") for financial support and S. Wiesner for assistance in thin film preparation.

[1]C. W. Tang, Appl. Phys. Lett. **48**, 183 (1986).
[2]R. Stein, F. R. Kogler, and Ch. Brabec, J. Mater. Chem. **20**, 2499 (2010).
[3]W. J. E. Beek, M. M. Wienk, and R. A. J. Janssen, Adv. Mater. **16**, 1009 (2004).
[4]K. M. Coackley, Y. Liu, M. D. McGehee, K. L. Frindell, and G. D. Stucky, Adv. Funct. Mater. **13**, 301 (2003).
[5]M. Kröger, S. Hamwi, J. Meyer, T. Riedl, W. Kowalsky, and A. Kahn, Appl. Phys. Lett. **95**, 123301 (2009).
[6]W. Riedel, S. Wiesner, D. Greiner, V. Hinrichs, M. Rusu, and M. Ch. Lux-Steiner, Appl. Phys. Lett. **104**, 173503 (2014).
[7]K. Koike, R. Wada, S. Yagi, Y. Harada, S. Sasa, and M. Yano, Jpn. J. Appl. Phys., Part 1 **53**, 05F J02 (2014).
[8]H. Simchi, B. E. McCandless, T. Meng, J. H. Boyle, and W. N. Shafarmann, J. Appl. Phys. **114**, 013503 (2013).
[9]V. Shrotriya, G. Li, Y. Yao, C. W. Chu, and Y. Yang, Appl. Phys. Lett. **88**, 073508 (2006).
[10]J. K. Larsen, H. Simchi, P. Xin, K. Kim, and W. N. Shafarmann, Appl. Phys. Lett. **104**, 033901 (2014).
[11]H. Bässler, Phys. Status Solidi B **175**, 15 (1993).
[12]P. W. M. Blom and M. C. J. M. Vissenberg, Mater. Sci. Eng. **27**, 53 (2000).
[13]V. I. Arkhipov *et al*., in *Semiconducting Polymers: Chemistry, Physics and Engineering*, 2nd ed., edited by G. Hadziioannou and G. Malliaras (Wiley-VCH Verlag, Weinheim, 2007).
[14]P. M. Borsenberger, Mol. Cryst. Liq. Cryst. **228**, 167 (1993).
[15]P. Pivrikas, M. Ullah, Th. B. Singh, C. Simbrunner, G. Matt, H. Sitter, and N. S. Sariciftci, Org. Electron. **12**, 161 (2011).
[16]P. M. Allemand, A. Koch, F. Wudl, Y. Rubin, F. Diederich, M. M. Alvarez, S. J. Anz, and R. L. Whetten, J. Am. Chem. Soc. **113**, 1050 (1991).
[17]B. P. Rand, J. Xue, S. Uchida, and S. R. Forrest, J. Appl. Phys. **98**, 124902 (2005).
[18]R. Könenkamp, G. Priebe, and B. Pietzak, Phys. Rev. B **60**, 11804 (1999).
[19]N. S. Sariciftci, L. Smilowitz, A. J. Heeger, and F. Wudl, Science **258**, 1474 (1992).
[20]P. Peumans, A. Yakimov, and S. Forrest, J. Appl. Phys. **93**, 3693 (2003).
[21]S. Sista, Y. Yao, and Y. Yang, Appl. Phys. Lett. **91**, 223508 (2007).
[22]A. Richter and J. Sturm, Appl. Phys. A **61**, 163 (1995).
[23]K. L. Mutolo, E. I. Mayo, B. P. Rand, S. R. Forrest, and M. E. Thompson, J. Am. Chem. Soc. **128**, 8108 (2006).
[24]H. Gommans, D. Cheyns, T. Aernouts, C. Girotto, J. Poortmans, and P. Heremans, Adv. Funct. Mater. **17**, 2653 (2007).
[25]A. J. Breeze, A. Salomon, D. S. Ginley, B. A. Gregg, H. Tillmann, and H.-H. Hörhold, Appl. Phys. Lett. **81**, 3085 (2002).
[26]M. Rusu, S. Wiesner, T. Mete, H. Blei, N. Meyer, M. Heuken, M. Ch. Lux-Steiner, and K. Fostiropoulos, Renewable Energy **33**, 254 (2008).
[27]M. Rusu, J. Gasiorowski, S. Wiesner, N. Meyer, M. Heuken, K. Fostiropoulos, and M. Ch. Lux-Steiner, Thin Solid Films **516**, 7160 (2008).
[28]L. Kronik and Y. Shapira, Surf. Sci. Rep. **37**, 1 (1999).
[29]I. Mora-Seró, Th. Dittrich, A. S. Susha, A. L. Rogach, and J. Bisquert, Thin Solid Films **516**, 6994 (2008).
[30]V. Duzhko, V. Yu. Timoshenko, F. Koch, and Th. Dittrich, Phys. Rev. B **64**, 075204 (2001).
[31]Th. Dittrich, S. Bönisch, P. Zabel, and S. Dube, Rev. Sci. Instrum. **79**, 113903 (2008).
[32]I. Mora-Seró, Th. Dittrich, G. Garcia-Belmonte, and J. Bisquert, J. Appl. Phys. **100**, 103705 (2006).
[33]V. Duzhko, F. Koch, and Th. Dittrich, J. Appl. Phys. **91**, 9432 (2002).
[34]S. Kobayashi, T. Takenobu, S. Mori, A. Fujiwara, and Y. Iwasa, Sci. Technol. Adv. Mater. **4**, 371 (2003).
[35]K. Itaka, M. Yamashiro, J. Yamaguchi, M. Haemori, S. Yaginuma, Y. Matsumoto, M. Kondo, and H. Koinuma, Adv. Mater. **18**, 1713 (2006).
[36]Z. Bao, A. J. Lovinger, and A. Dodabalapur, Appl. Phys. Lett. **69**, 3066 (1996).
[37]F. E. Osterloh, M. A. Holmes, L. Chang, A. J. Moulé, and J. Zhao, J. Phys. Chem. C **117**, 26905 (2013).
[38]F. E. Osterloh, M. A. Holmes, J. Zhao, L. Chang, S. Kawula, J. D. Roehling, and A. J. Moulé, J. Phys. Chem. C **118**, 14723 (2014).